

United States
Department of
Agriculture

Forest Service

Forest
Products
Laboratory

General
Technical
Report
FPL-27
1979

Stress-Wave Grading Techniques on Veneer Sheets

Abstract

A study was conducted to compare stress wave devices and determine the information available from stress waves in veneer sheets. The distortion of the stress wave as it passed a defect indicated that an estimate of the location and size of the defect can be obtained but information regarding wood quality is lost in the areas immediately behind a knot.

KEYWORDS Wood, veneer, stress wave, defects, nondestructive testing.

STRESS-WAVE GRADING TECHNIQUES ON VENEER SHEETS

By

JOSEPH JUNG, General Engineer

ForestProductsLaboratory,¹ ForestService

US. Department of Agriculture

Introduction

Perhaps one of the most useful characteristics of parallel laminated veneer (PLV) and related products such as Forest Products Laboratory's Press-Lam (8,9,10)² is that it is comprised of several distinct layers of material. Not only does this layering decrease the variability in some strength properties by minimizing the influences of the defects, but it also provides the PLV producer with an opportunity to construct his product from material of known or estimated quality. This fact may allow for the production of PLV with varying degrees of performance depending on the required characteristics of the end products.

The key to this concept, of course, would be the accurate assessment of the quality of each piece of veneer. This investigation focused on the use of stress wave techniques (5-8) for this purpose. Although the application of these techniques to estimate veneer quality (primarily Young's modulus, slope of grain, and knots) is not new, its application to veneer sheets wider than approximately 3 inches has not been reported on in past literature. This investigation was an effort to determine what information regarding veneer quality could be ascertained through stress-wave testing in the direction of the grain.

This study was designed to evaluate different techniques and devices that could be used in the stress-wave testing of wide veneer pieces. As part of the evaluation, it was hoped that information, such as the devices' ability to detect defects and to provide an overall estimate of the veneer quality, would be obtained.

Methods

Material

The material used for this study consisted of 15 sheets of rotary-peeled red oak veneer, approximately 4 feet by 10 inches by 0.25 inch. The veneers were press dried to approximately 12 percent moisture content and then stored at 74° F, 65 percent relative humidity for over 1½ months prior to testing. The veneers were chosen to represent a variety of defect sizes and locations. A summary of the veneers' physical properties is given in table 1.

Equipment

The stress-wave devices and their associated accelerometers and transducers used in this study were the Washington State University (WSU) impact stress-wave equipment and its accelerometers (figure 1) and the James V-Meter and its 50 kHz piezoelectric transducers (fig. 2). Both of these devices measure the time required for a stress wave to travel between two points (transit time). In part of this study, the James V-Meter device was used with the WSU device accelerometer as its signal receiver. Thus, three combinations of devices were used in this study:

- Device 1. WSU stress-wave machine.
- Device 2. James V-Meter.
- Device 3. James V-Meter using a WSU accelerometer as its receiver.

A heavy grease couplant was used with Device 2 transmitter and receiver, and Device 3 sender.

Experimental Procedures

Veneer physical properties. – The dimensions, weight, and slope of grain on the tight faces (the sides without the knife checks) of each veneer were

measured and recorded. The slope of grain was measured by scribing a mark in the grain over a distance of approximately 1 foot. The average angle of the scribe mark with respect to longitudinal axis of the piece (counterclockwise is positive) was taken as the slope of grain (table 1).

Stress wave testing of full width specimens.

– The 10-inch-wide specimens (fig. 3) were subjected to stress-wave testing both with the transmitter and receiver located on the end grain, and with the transmitter on the end grain and the receiver located at some point on the interior of the veneers.

The veneers were marked with a 3-by 1-inch grid (fig. 4). A coordinate system was used, with the bottom left corner of the veneers being the origin. The sender was always positioned at the left end of the veneer at one of the row lines. The receiver, for end-grain stress-wave readings, was placed on one of the row lines at the right end of the veneer. For interior stress-wave readings, the receiver was placed on the grid line intersection points.

For the end-grain stress-wave testing, two test modes—methods of locating the sender and receiver—were used. In Mode 1, the sender was placed on the left end at the middle of the veneer piece (row 5) and transit time readings were taken with the receiver positioned at the right end of the veneers at rows 1, 3, 5, 7, and 9. In Mode 2, the sender was placed

¹Maintained at Madison, Wis., in cooperation with the University of Wisconsin.

²Underlined numbers in parentheses refer to literature cited at end of report.

Table 1.–Veneer properties

Veneer No.	Length	Width	Average thickness	Weight	Slope of grain	Mass density
	In.	In.	In.	Lb	Degrees	$\frac{(\text{Lb-sec}^2)}{\text{in.}^4} \times 10^{-5}$
A- 1	49.1	10.0	0.275	2.99	4.0	5.74
A- 2	49.8	10.0	.274	2.97	0.	5.63
A- 3	48.4	10.0	.289	3.11	0.	5.75
A- 4	48.4	9.97	.275	2.93	-2.5	5.71
A- 5	49.5	10.0	.269	2.63	0.5	5.12
A- 6	48.7	10.0	.278	2.98	0.0	5.69
A- 7	49.3	9.97	.271	2.76	6.	5.37
A- 8	49.6	10.0	.275	2.85	4.5	5.40
A- 9	49.3	10.0	.274	2.80	0.	5.36
A-10	49.6	9.97	.273	2.92	-1.	5.60
A-11	49.3	10.0	.270	2.84	4.	5.53
A-12	49.6	10.0	.264	2.65	-2.	5.23
A-13	49.0	10.0	.277	2.98	6.	5.68
A-14	49.2	10.0	.277	2.93	-0.5	5.57
A-15	49.5	10.0	.274	2.88	0.	5.49

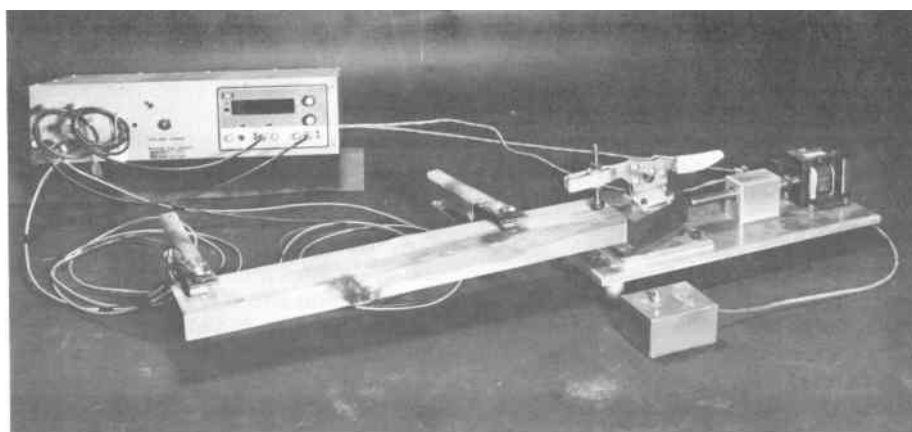


Figure 1.–WSU Stress-wave device (Device 1). (M 141 881)

consecutively at rows 1, 3, 5, 7, and 9 on the left end of the veneers, and the receiver was placed at the right end of the specimens at the same row number—i.e., the sender was placed at the left end of row, and the receiver at the right end of row, (i = 1, 3, 5, 7, 9).

Devices 1 and 2 were used in both modes to record end-grain stress-wave transit times.

Device 3 was used to obtain stress-wave transit times at interior points in the veneers. Using the WSU accelerometer facilitated obtaining stress-wave transit times at the interior points because the accelerometers are relatively small. The transit time readings were taken in a fashion similar to Mode 2 described above, but in this case the sender was, held on one of the

nine rows at the left end of the veneers as the receiver was moved to each of the 16 column points on that row. This process was repeated on each row of each veneer.

Determination of stress-wave velocity as a function of angle to the grain.

— One veneer, A-13, was chosen for its visual clearness and uniformity to be tested with Device 3. The sender was placed at the left end of row number 5, and transit time readings were taken at the 144 row and column intersection points of the grid marked on the specimen.

Stress-wave test on strips. — For the final series of tests, each veneer was ripped into approximately 2-inch-wide

strips—i.e., along rows 2, 4, 6,8 (fig. 5). Each strip was tested with Device 2 using the Mode 2 test configuration.

Data Reducfion Procedures

Calculation of wave velocity. — The calculation of the stress-wave velocity from transit time data taken at the veneer end grain was performed by dividing the straight line distance between the sender and receiver by the measured transit time. The calculation of the wave velocity between two interior points which lie on the same row was taken as the distance between the two points divided by the change in transit time readings between the points.

Construction of transit time contour mapping. — Stress-wave transit times in the interior of the veneers were contour plotted through the use of a computer program (3).

Construction of wave velocity surfaces. — The stress-wave velocities in the veneers were plotted as a function of their position on the veneer surfaces. The velocities were calculated at the intersections of the 9 rows and 16 columns (fig. 6) and were later refined by linear interpolation (1); the resulting arrays were then smoothed and plotted as three dimensional surfaces (1,2).

Results and Discussion

Comparison of Stress-Wave Devices

To obtain a comparison between the results that could be expected from the stress-wave devices used in this study, the velocities of the stress waves from receiver locations 1, 3, 5, 7, and 9 were compared three ways: (1) Device 1 against Device 2, both using a Mode 1 sender configuration; (2) Device 1 against Device 2, both using a Mode 2 sender configuration; and (3) Device 3 against Device 2, both using the Mode 2 configuration. Device 2 was used as a basis for comparison as it appeared to provide the most repeatable results. The differences of the velocities were expressed as a percentage of the Device 2 velocity.

The stress-wave velocities obtained from Device 1 are, on the average (table 2), approximately 7.9 percent lower than those obtained from using Device 2. This difference appears to be independent of the sender location (Mode 1 versus Mode 2).

The comparison between Devices 3

and 2 showed that the velocities obtained for Device 3 are approximately 3 percent lower than those obtained from Device 2. The standard deviation is about one half of that obtained from the Mode 2 comparison between Devices 1 and 2.

In general, the differences between all the devices are relatively small (maximum mean difference of about 8 pct). Thus, comparable conclusions could be reached from the results of any of the devices. But it should be noted that an impact device, such as Device 1, requires securing (clamping) the specimen at the impact area. This is a relatively slow procedure compared to that used for Devices 2 and 3 where only firm physical contact with an appropriate couplant is required to transmit and receive the wave.

Effect of Slope of Grain

Stress-wave velocities in specimen A-13 are plotted as a function of the angle to the grain (fig. 6). Strictly speaking, this may not be a true plot of wave velocity versus angle to the grain for higher angles to the grain, because the wave may be affected by the edge of the veneer. If we consider only small angles, however, it is apparent that the stress-wave velocities decrease rapidly as the angle of the reading deviates from that of the grain. It is estimated (from fig. 7) that an angle of 5 degrees to the grain will yield velocities approximately 4 percent less than a zero degree reading; readings at an angle of 10 degrees to the grain will yield a 19 percent decrease. These figures imply that at small angles to the grains (0 to 5 degrees) the stress-wave readings are relatively insensitive, but at slightly larger angles, the stress-wave readings could be significantly affected.

Transit Time Contours and Wave Velocity Surfaces

Transit time contours. – Selected transit time contour plots from the Device 3 testing (figs. 7-9) yield three main observations:

1. Knots impede the propagation of the stress waves,
2. Diving grain (sharp grain angles to the faces of the veneers) is not readily detected, and
3. After the wave has been slowed by a defect, the wave tends to catch up to itself—i.e., the impeded portion of the wave "appears" to have a higher forward velocity than the other portions of the wave after it passes the defect.

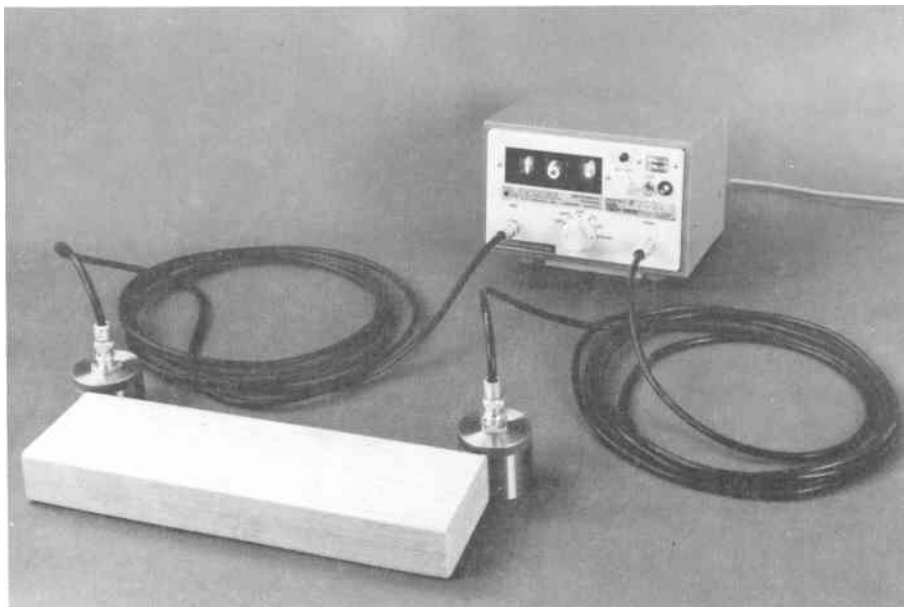


Figure 2.—James V-Meter (Device 2). (M 143 888)

Table 2.—Comparison of the wave velocities of the stress wave devices

Description of comparison	Sender mode	Mean percent difference	Standard deviation
		<u>Pct</u>	<u>Pct</u>
$\frac{\text{Device 1-Device 2}}{\text{Device 2}} \times 100$	1	-7.88	4.62
$\frac{\text{Device 1-Device 2}}{\text{Device 2}} \times 100$	2	-7.88	3.09
$\frac{\text{Device 3-Device 2}}{\text{Device 2}} \times 100$	2	-2.97	1.68

This apparent high-wave velocity is probably fictitious.

Knots in the veneer pieces consistently retarded the wave front as it passed. This, of course, would be expected because the wave travels faster with the grain than across it, as it does when it passes through a knot. This effect is readily apparent in the contour plots of transit times.

A good illustration of the effects of knots on the contour plots of the wave form is the distinct distortion of the wave in the center of the plot for specimen A-2 (fig. 8). The actual knot begins at a distance of approximately 22 inches from the left end of the specimen, the location at which distortion of the stress wave begins to

become pronounced.

Diving grain is not readily detected by the stress-wave testing procedures used. It would be intuitively expected that in areas where the grain makes a sharp angle to the face of the veneer, the measured transit times would be different than if the grain were at a small angle to the surface. From the contour plot for specimen A-2 (fig. 8) this is apparently not the case. In the upper left corner of this specimen, is a substantial amount of diving grain (1/6.4 slope), but the contour plot shows no variation in wave shape. The same is true for specimen A-4 (fig. 9) (1/7.3 slope) at coordinates of X » 20 inches, Y » 3 inches.

After a wave passes a knot, the

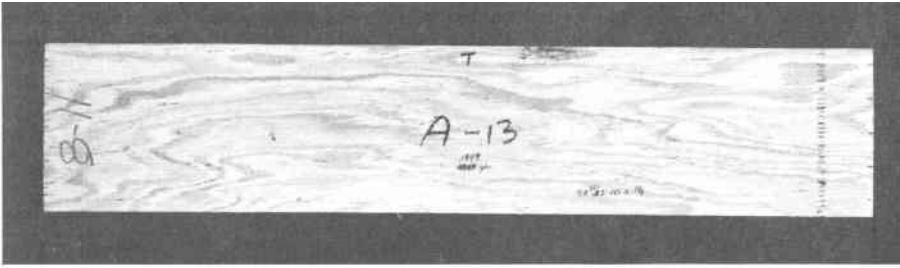


Figure 3.—Veneer A-13, a rather clear, but otherwise typical, specimen. (M 145011)

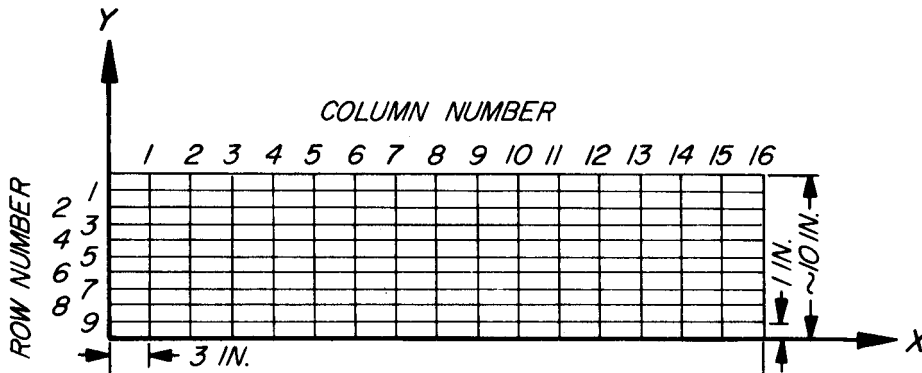


Figure 4.—Grid orientation for veneers. (M 148 081)

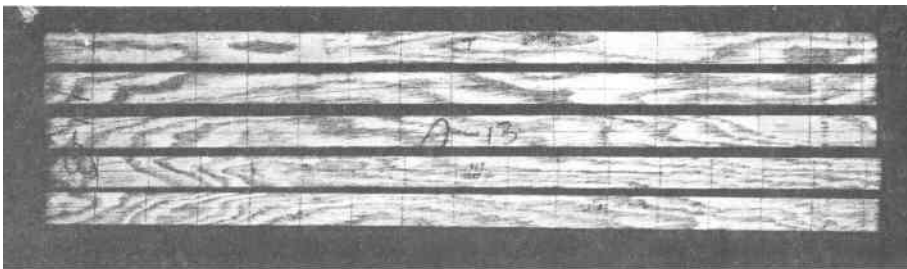


Figure 5.—Veneer A-13 cut into 2-inch strips. (M 145284)

retarded wave "appears" to catch up to the entire wave front. This is illustrated in most of the contour plots but is particularly noticeable in the plots for specimens A-1, A-2, and A-4, (figs. 7-9). Apparently, the wave propagates into the retarded wave areas in a direction transverse to the assumed direction of travel which is parallel to the longitudinal axis of the veneer. This fact may limit the amount of information available from stress-wave testing if readings are taken only at the ends of the veneers: even though the wave is

greatly retarded when it passes a knot, it may not be retarded significantly by the time it reaches the signal receiver at the end of the veneer.

Wave velocity surfaces. — From the wave velocity surfaces (figs. 7-9), it is possible to conclude that there is a decrease in wave velocity as the wave passes a knot. The wave velocity in the large knot area of specimen A-2 was approximately 0.05 inch per microsecond (in./ μ sec), and an estimate of the average velocity in the

clear wood would be about 0.155 in./ μ sec. This difference is approximately of the magnitude which would be expected between the velocities of waves traveling perpendicular to and along the grain (11). Similar results can be observed in the velocity surfaces of the other specimens.

Perhaps the most noticeable features of the velocity surfaces are the high sharp peaks. These peaks, in general, are in the areas behind the knots. As mentioned, the wave front apparently first propagates into these areas from portions of the stress wave which passed along the side of the knots. Because of this and the fact that in the calculation of the wave velocities, it was assumed that the wave travels parallel to the longitudinal axis of the veneer; these plots show artificially high velocities in these areas. If it were not for these peaks in the velocity surfaces, a good estimator of the veneer quality could possibly be the volume under the velocity curves.

End-Grain Stress-Wave Results

As might be expected, stress-wave results can be significantly affected by the angle of the sender-receiver line to the direction of the grain. Mode 1 testing exacerbated this effect. Consequently, only the results of Mode 2 testing are reported here.

Comparison of stress-wave tests on sheets and strips. — Stress-wave readings on 10-inch-wide veneer sheets as opposed to 2-inch strips were compared by percentage differences (fig. 5) (table 3).

From the results of the essentially clear pieces of veneer, specimens A-10, A-13, and A-15, the variations between the readings taken on the specimens when they were 10 inches wide and after they were cut appear to be approximately $\pm 6 \mu$ sec. The average transit time for the stress wave was approximately 200 μ sec. Thus, a $\pm 6 \mu$ sec variation would be about a ± 3 percent deviation in the results of the clear wood specimens.

Assuming that in clear pieces, the effects of testing the wood in strips or sheets are negligible, this ± 3 percent variation would appear to be a measure of the repeatability of results. Thus, differences in results outside this range would be indicative of the effects of testing strips versus sheets.

This comparison (table 3) is, in

general, indicative of the notion that the width of the veneer affects the average velocity of the stress waves. The results for the strips of veneer with knots showed significant increases in wave transit times over those taken at the same location but while the veneers were 10 inches wide. Good examples for this observation are the results for specimens A-2, A-3, and A-4. A similar conclusion could be deduced from the contour plot data discussed earlier.

Somewhat puzzling results for specimen A-6 at row 7 and specimen A-8 at row 1 (table 3) should be noted. At these positions, the average velocities of the waves were apparently higher in the strips than in the sheets. It would normally be thought that the average velocities would be highest in the sheets because the waves have more medium to propagate through and to reduce the effects of the defects. No explanation has been developed for these results.

Estimation of veneer quality from end-grain results. — Although stress-wave results are highly affected by the width of the specimens, it is conceivable that an overall estimate of the quality of wider pieces of veneer can still be obtained. To determine what sorting decisions end-grain stress-wave testing on veneer sheets would yield, the veneers were ranked (table 4) in ascending order of predicted quality by means of average wave velocities from the nine rows (assuming higher velocity implies higher quality) and the predicted Young's modulus, $E = rv^2$, using average velocities and gross densities. This compilation was performed for the Mode 2 testing for Devices 1 and 2.

General observations are that the low-quality, highly defective materials were low on this list—e.g., specimens A-7, A-8, A-9—and that clear straight grain materials were high on the lists—e.g., A-1, A-10, and A-15. Similar but not identical conclusions could be made by using only the center stress-wave reading. The ability to discriminate between high and low quality material is apparently not greatly enhanced by using $E = rv^2$ and may not warrant the added work of obtaining the density.

Similar conclusions for the veneer strips can also be reached. The strips were also ranked in ascending order relative to the average wave velocity from end to end (table 5) and their predicted modulus of elasticity (table 6). It appears that the technique of stress-waving veneers to obtain estimates of quality becomes more discriminating as

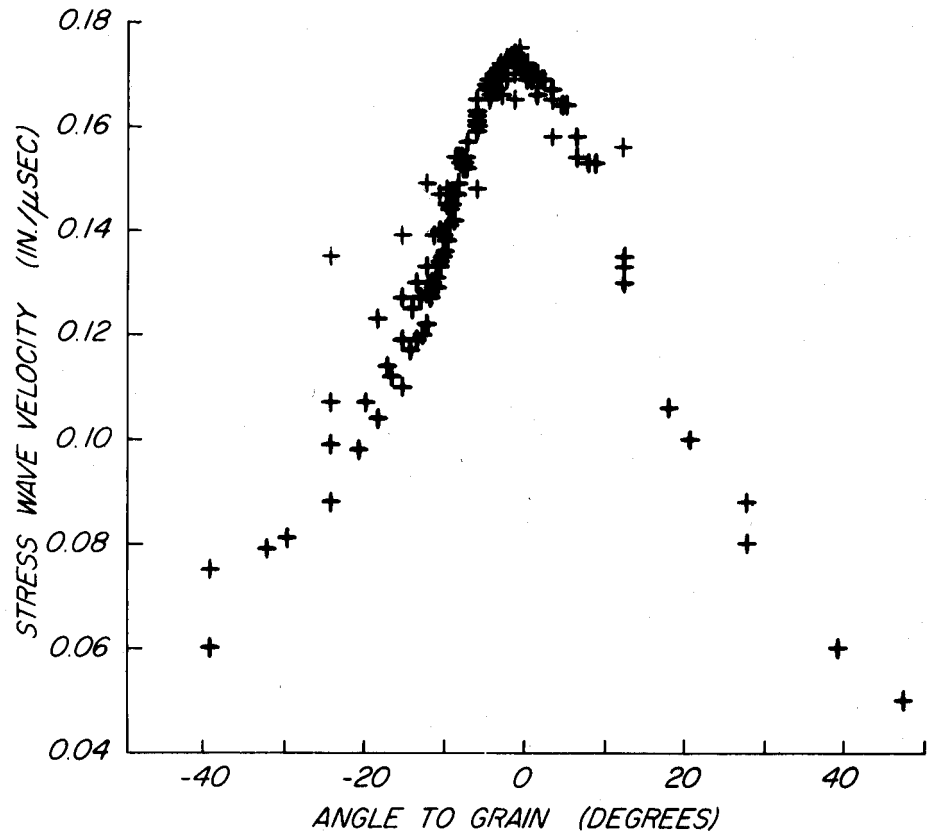


Figure 6.—Stress-wave velocity as a function of the angle of the grain in specimen A-13.
(M 148 082)

the pieces become narrower.

It must be noted, though, that because the size and the location of knots affect end-grain stress-wave results, readings taken on veneers with knots close to the receiver may yield very false estimates of the veneer quality.

Conclusions

The major conclusions which could be drawn are:

1. A comparison of the devices used in the study showed that the results were within 8 percent of one another.
2. The wave velocities can be highly affected by the angle between the slope of the grain and the sender-receiver line if the angle is more than about 5 degrees.
3. Sharp grain angles to the faces of the veneer (diving grain) were not detected by the stress-wave techniques used in this study.
4. Stress waves are impeded as they pass through knots, but on wide veneers the delayed portion of the wave appears to "catch up" with the remaining portion of the wave after the defect is passed.
5. With the signal sender placed on the end grain of the veneers and by recording transit time data at interior veneer points, the defect locations can be ascertained but information is lost in "shadow areas" behind the knots.
6. By taking stress-wave readings at end grain positions only, it is unlikely that information regarding the size and location of defects can be ascertained. Also, the results appear to indicate that the narrower the veneer pieces, the better the stress-wave estimate of veneer quality because the wave path is more restricted.

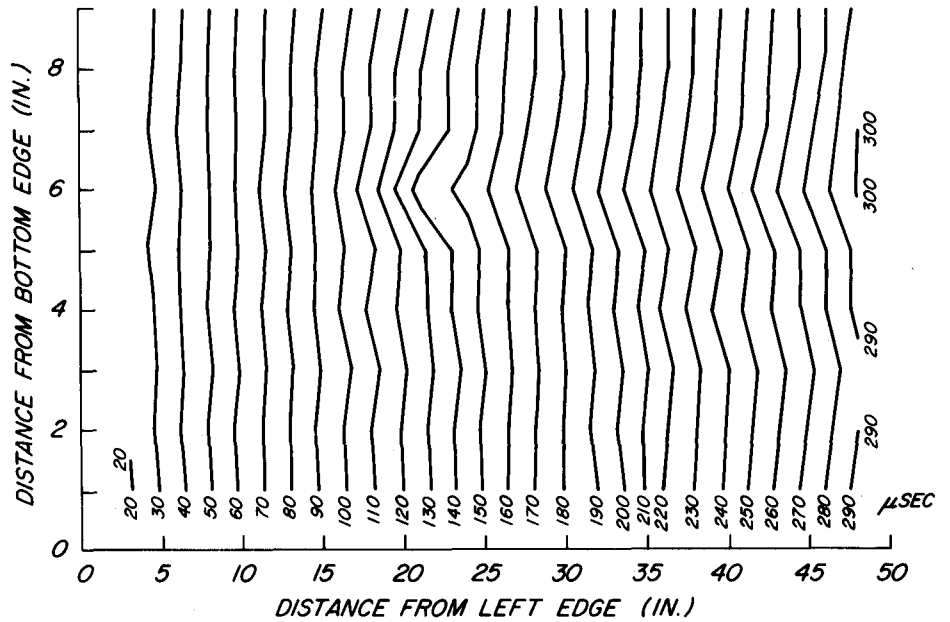
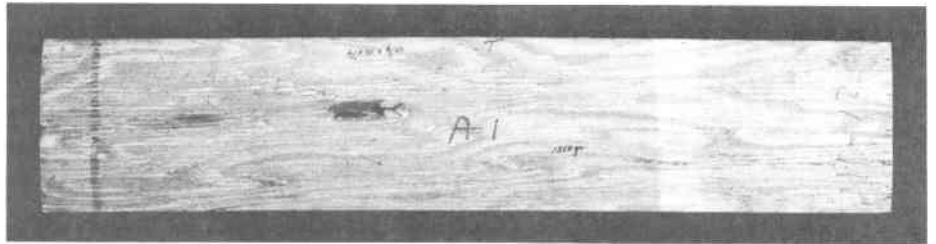
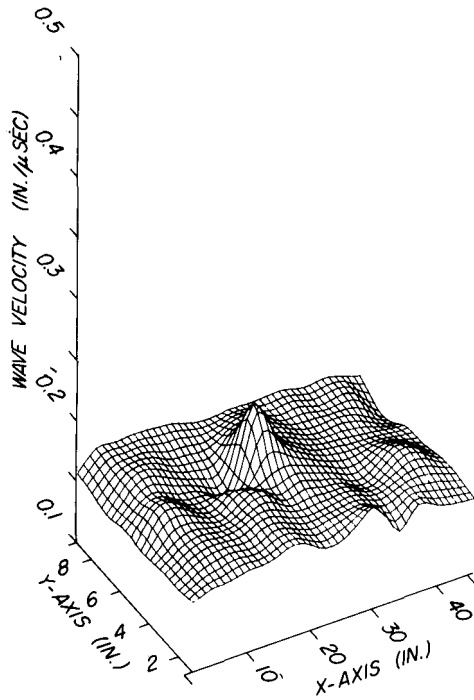


Figure 7.—Specimen A-1, its transit time contours, and its wave velocity surface.
 (M 145 009)
 (M 148 088)
 (M 148 085)

Table 3.—Percentage difference between Device 2 transit time reading on veneer strips and 10-inch-wide sheets¹ at selected positions

Veneer No.	Row number				
	1	3	5	7	9
%.....				
A- 1	3.77	-0.669	-0.683	0.692	1.71
A- 2	7.24	0.	3.74	1.99	-1.69
A- 3	14.10	6.80	-3.41	6.00	1.66
A- 4	.344	12.4	-.662	-.336	-1.36
A- 5	0.	1.42	-.671	-.635	0.
A- 6	.331	.340	18.3	-6.95	4.21
A- 7	² 6.33	³ -	2.13	0.	-1.19
A- 8	-2.80	28.3	3.67	-.305	-.295
A- 9	3.17	³ -	.298	2.39	2.70
A-10	.362	.719	-1.718	-1.35	2.06
A-11	1.05	-1.33	1.36	-1.36	2.71
A-12	0.	0.	1.31	-1.55	1.64
A-13	2.05	-.347	.676	-1.55	1.64
A-14	.697	-.671	-.637	-.680	.699
A-15	4.80	-.690	-.699	-.344	.333

$$^1\text{Percentage difference} = \frac{(\text{Stress wave reading on 2-inch strip}) - (\text{Stress wave reading on 10-inch sheet})}{\text{Stress wave reading on 10-inch sheet}} \times 100$$

²Veneer strip was broken but was physically held together at the time the reading was taken.

³Veneer strip was too badly broken to take reading.

Table 4.—Ranking of veneers in ascending order of stress wave predicted quality

Device 1				Device 2			
Sorting based on average velocity		Sorting based on E		Sorting based on average velocity		Sorting based on E	
Veneer No.	Average velocity In./μsec.	Veneer No.	Young's modulus Million psi	Veneer No.	Average velocity In./μsec.	Veneer No.	Young's modulus Million psi
7	0.129	7	0.894	7	0.144	7	1.11
8	.131	8	0.927	9	.149	9	1.19
9	.138	9	1.02	8	.150	8	1.22
3	.149	12	1.11	3	.161	12	1.36
6	.149	5	1.23	12	.161	5	1.38
12	.151	6	1.26	4	.162	3	1.49
13	.151	3	1.28	6	.163	4	1.50
2	.152	2	1.30	5	.164	14	1.53
4	.152	13	1.30	13	.166	6	1.53
11	.154	11	1.31	14	.166	11	1.54
1	.155	4	1.32	11	.167	2	1.57
5	.155	14	1.34	2	.167	13	1.59
14	.155	15	1.37	1	.168	15	1.59
15	.158	1	1.38	15	.170	1	1.62
10	.162	10	1.47	10	.173	10	1.68

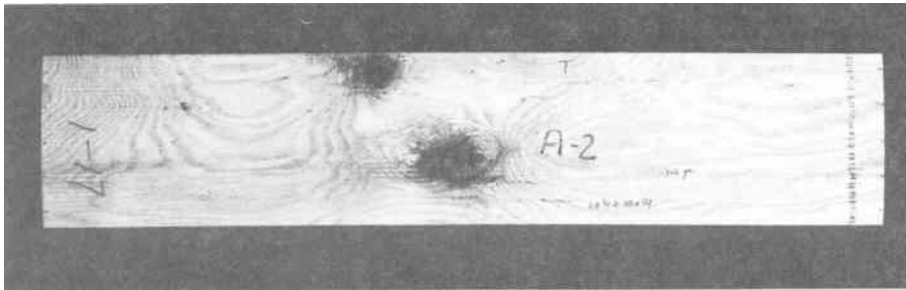
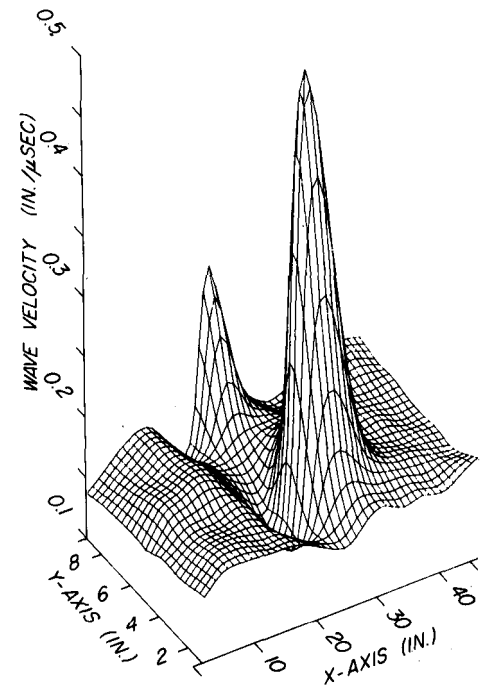
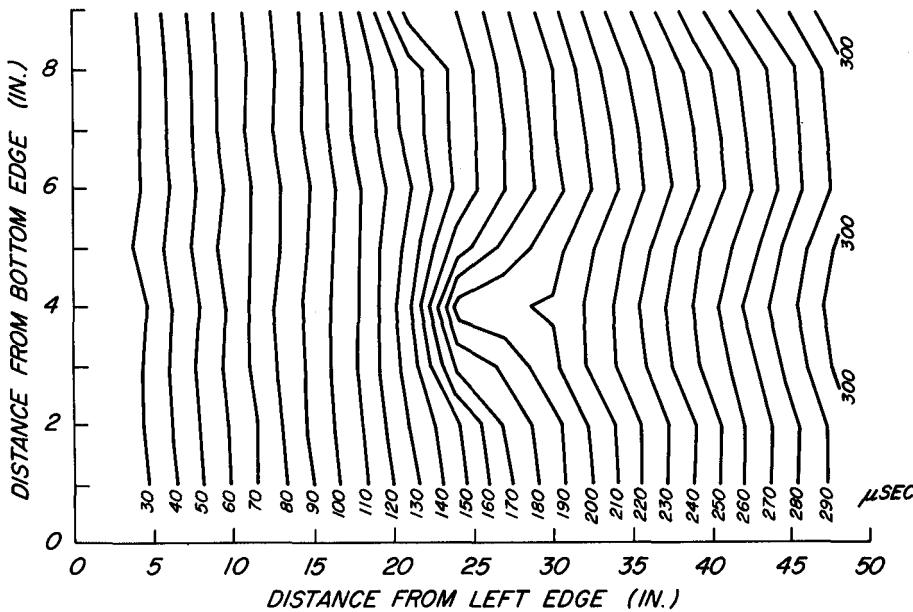


Figure 8.—Specimen A-2, its transit time contours, and its wave velocity surface.
(M 145 009)
(M 148 087)
(M 148 084)



M 148 084

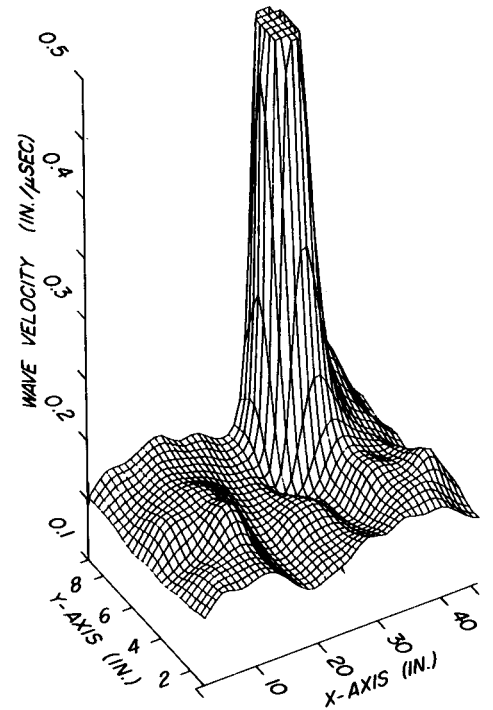
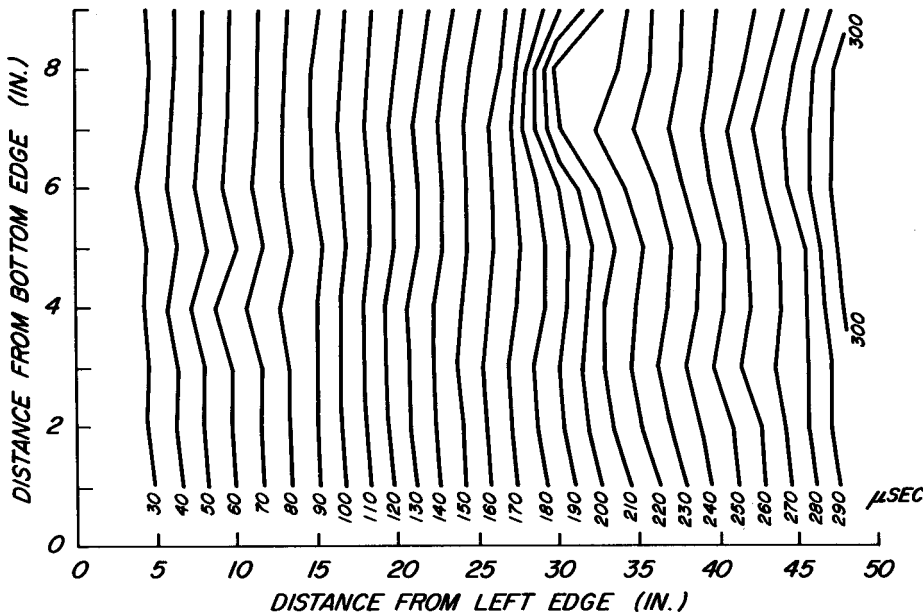
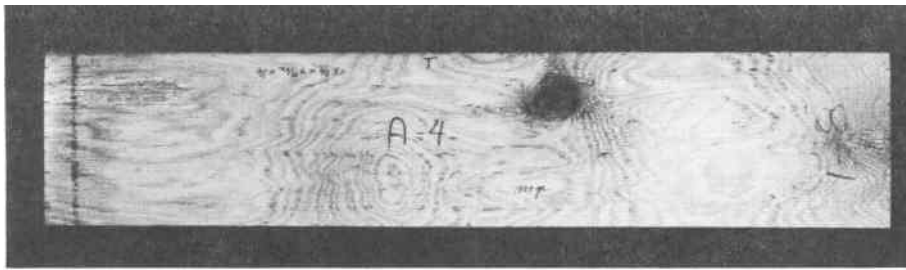


Figure 9.—Specimen A-4, its transit time contours, and its wave velocity surface.
(M 145 009)
(M 148 086)
(M 148 083)

Table 5—Ranking of veneer strips¹ in ascending order according to average wave velocity

Veneer and strip No.	Average wave velocity	Veneer and strip No.	Average wave velocity	Veneer and strip No.	Average wave velocity	Veneer and strip No.	Average wave velocity	Veneer and strip No.	Average wave velocity
	In./μsec		In./μsec		In./μsec		In./μsec		In./μsec
A-7-2	² —	A- 7-4	0.149	A-12-3	0.161	A- 1-2	0.165	A- 2-2	0.170
A-9-2	² —	A- 9-1	.151	A- 1-1	.162	A- 1-5	.165	A-11-1	.170
A-7-1	0.122	A- 3-4	.152	A- 2-4	.162	A- 5-3	.165	A-14-1	.170
A-8-2	.122	A- 8-4	.152	A- 4-5	.162	A- 6-2	.165	A-13-2	.171
A-6-3	.132	A- 2-1	.153	A-12-1	.162	A-10-5	.165	A-14-5	.171
A-3-1	.136	A- 3-2	.154	A-12-2	.162	A-11-3	.165	A-15-4	.171
A-4-2	.141	A-12-4	.156	A-15-1	.162	A- 3-3	.166	A- 2-5	.172
A-9-4	.144	A- 5-4	.157	A- 2-3	.163	A- 4-1	.166	A- 5-1	.172
A-9-5	.144	A- 3-5	.158	A- 4-4	.163	A-13-4	.166	A-10-3	.172
A-8-3	.146	A-14-3	.158	A-11-5	.163	A-11-2	.167	A-15-2	.172
A-9-3	.146	A- 8-1	.159	A- 6-5	.164	A-14-4	.168	A- 6-4	.173
A-7-3	.146	A-13-5	.159	A-13-1	.164	A- 1-3	.169	A-15-3	.174
A-0-5	.147	A-12-5	.160	A-13-3	.164	A- 1-4	.169	A-10-2	.176
A-7-5	.148	A- 4-3	.161	A-14-2	.164	A-10-4	.169	A- 5-2	.178
A-5-5	.149	A- 6-1	.161	A-15-5	.164	A-11-4	.169	A-10-1	.178

¹Each column gives the original veneer number and the strip number (1 denotes top and 5 denotes bottom of the veneer).

²Veneer strip was broken.

Table 6.-Ranking of veneer strips¹ in ascending order according to predicted "E"

Veneer and strip No.	Predicted "E"	Veneer and strip No.	Predicted "E"	Veneer and strip No.	Predicted "E"	Veneer and strip No.	Predicted "E"	Veneer and strip No.	Predicted "E"
	Million <u>psi</u>		Million <u>psi</u>		Million		Million <u>psi</u>		Million <u>psi</u>
A-7-2	² -	A- 7-4	1.19	A- 3-5	1.44	A- 65	1.53	A-15-4	1.60
A-9-2	² -	A- 9-1	1.23	A-13-5	1.44	A-10-5	1.53	A-14-1	1.61
A-8-2	0.79	A- E4	1.24	A-15-1	1.44	A-11-2	1.53	A- 5-2	1.62
A-7-1	.80	A- 5-4	1.26	A-11-5	1.46	A-13-1	1.53	A-15-2	1.62
A-6-3	.99	A-12-4	1.28	A- 61	1.47	A-13-3	1.54	A- 1-3	1.63
A-3-1	1.06	A- 3-4	1.33	A- 4-3	1.49	A- 62	1.55	A- 1-4	1.63
A-9-4	1.11	A- 2-1	1.34	A-15-5	1.49	A- 1-2	1.57	A-14-5	1.63
A-9-5	1.11	A-12-5	1.34	A- 2-4	1.50	A- 1-5	1.57	A- 2-2	1.66
A-4-2	1.12	A-12-3	1.35	A- 4-5	1.50	A- 4-1	1.57	A-10-3	1.66
A-5-5	1.14	A- 3-2	1.37	A-11-3	1.50	A-13-4	1.57	A-13-2	1.66
A-9-3	1.15	A- E1	1.31	A-14-2	1.50	A- 3-3	1.58	A-15-3	1.67
A-7-3	1.16	A-12-1	1.37	A- 1-1	1.51	A-14-4	1.58	A- 2-5	1.69
A-8-3	1.16	A-12-2	1.37	A- 4-4	1.52	A-11-4	1.59	A- 64	1.71
A-E5	1.16	A- 5-3	1.39	A- 5-1	1.52	A-10-14	1.60	A-10-2	1.74
A-7-5	1.18	A-14-3	1.40	A- 2-3	1.53	A-11-1	1.60	A-10-1	1.17

¹Each column gives the original veneer number and the strip number (1 denotes top and 5 denotes bottom). Veneer strip was broken.

Literature Cited

1. Academic Computing Center, University of Wisconsin-Madison.
1973. Two dimensional interpolation smoothing and refining.
December. Univ. Wis., Madison, Wis.
2. Academic Computing Center, University of Wisconsin-Madison.
1976. Surgen—three-dimensional surface generator, March. Univ. Wis.,
Madison, Wis.
3. Academic Computing Center, University of Wisconsin-Madison.
1977. Contr and contra—contourgraphing routines. April. Univ. Wis.,
Madison, Wis.
4. FPL Press-Lam Research Team.
1976. Press-Lam: Progress in technical development of laminated
veneer structural products. USDA For. Serv. Res. Pap. FPL 279. For.
Prod. Lab., Madison, Wis.
5. Gailigan, W. L., and R. Courteau.
1965. Measurement of elasticity of lumber with longitudinal stress waves
and the piezoelectric effect of wood. Proc. 2nd Symp. Non-
Destructive Testing of Wood, p. 223-244. Wash. State Univ., Pullman,
Wash.
6. Koch, Peter.
1967. Location of laminae by elastic modulus may permit manufacture
of very strong beams from rotary-cut southern pine veneer. U.S. For.
Serv. Res. Pap. SO-30. So. For. Exp. Stn., New Orleans, La.
7. Koch, Peter, and G. E. Wooden.
1968. Laminating butt-jointed, log-run southern pine veneers into long
beams of uniform high strength. For. Prod. J. 18(10):45-51.
8. McAlister, Robert H.
1976. Modulus of elasticity distribution of loblolly pine veneer as related
to location within the stem and specific gravity. For. Prod. J.
26(10):37-40.
9. Moody, R. C., and C. C. Peters.
1972. Feasibility of producing a high-yield laminated structural product:
Strength properties of rotary knife-cut laminated southern pine.
USDA For. Serv. Res. Pap. FPL 178. For. Prod. Lab., Madison, Wis.
10. Schaffer, E. L., R. W. Jokerst, R. C. Moody, and others.
1972. Feasibility of producing a high-yield laminated structural product:
General summary. USDA For. Serv. Res. Pap. FPL 175. For. Prod.
Lab., Madison, Wis.
11. U.S. Department of Agriculture, Forest Service, Forest Products Laboratory.
1974. Wood Handbook: Wood as an engineering material. U.S. Dep.
Agric., Agric. Handb. 72 (Rev.). USDA, Washington, D.C.